Engineering Solid Mechanics 10 (2022) 311-324

Contents lists available at GrowingScience

Engineering Solid Mechanics

homepage: www.GrowingScience.com/esm

Mathematical modelling for multiple straight cracks with coalesced yield zones

Naved Akhtar[a*], S. Hasan[b] and S. Shekhar[b]

[a]*Department of Applied Sciences and Humanities, Jamia Millia Islamia (A central University), New Delhi-110 025, India*
[b]*Department of Mathematics, Jamia Millia Islamia, New Delhi-110 025, India*

ARTICLE INFO

Article history:
Received 8 January 2022
Accepted 22 June 2022
Available online
22 June 2022

Keywords:
Dugdale model, Crack-tip opening displacement (CTOD)
Collinear cracks
Complex variable method
Stress intensity factor
Multi-site damage problem
Unified yield zones

ABSTRACT

Solution for a normally loaded infinite isotropic plate containing five cracks with coalesced yield zones is obtained using a complex variable method. Influence of coalesced yield zones on the load bearing capability of the infinite plate is analyzed. Analytical expressions for stress intensity factors, displacement components and crack opening displacement (COD) are obtained. Numerical study is carried out to determine the yield zone length, applied load ratio and COD. The numerical results are reported graphically between some important parameters.

1. Introduction

The problem of yield zones coalescence has not received extensive theoretical treatment in fracture mechanics yet. The large multi-site damage (MSD) problem has been discussed without considering this effect. The subject of eventual concern therefore is to study the effect of coalesced yield zones on the load bearing capability of the structures. Multi-site damage is a big concern for the integrity and durability of the life-dependent structures like aircraft, buildings, bridges, etc. (Swift, 1994). Various accidents have taken place in the past due to decreasing residual strength of engineering materials on the sudden link-up of several small cracks (Findlay & Harrison, 2002). Thus, the fracture mechanics-based analysis of these structures is important for their safe operations (Liu et al., 2019).

The main objectives of the fracture mechanics-based analysis are to determine the stress intensity factor (SIF), size of yield zones, crack-tip opening displacement (CTOD), energy release rate etc. Various analytical and numerical methods have been suggested to evaluate these parameters for MSD problems in finite and infinite plates, but the approach of Dugdale (1960) and Barenblatt (1962) has been found worthy in the modeling of such problems due to its mathematical simplicity. Closed form expressions of the yield zone length at the tips of a single crack in a sheet and the crack opening displacement for the same configuration examined experimentally by Burdekin et al. (1966). Also, for linearly varying stress distribution Kanninen (1970) and non-linear stress distribution by Harrop (1978).

Vast applicability of Dugdale-Barenblatt model for single crack problem, motivated various researchers to extended the idea to solve multiple crack problems. Some of them are, Theocaris (Theocaris, 1983) extend the model to solve the problem of two unequal/equal collinear straight cracks in an infinite plate. The results of Theocaris was further modified by Collins and Cartwright (2001). Xu et al. (2011) used a weight function approach to model the problem of two equal collinear straight

* Corresponding author.
E-mail addresses: naved.a86@gmail.com (N. Akhtar)

doi: 10.5267/j.esm.2022.6.006

cracks in an infinite sheet and also for three collinear cracks (Xu & Wu, 2012). A complex variable method was used by Hasan and Akhtar (2015) to obtain the yield zone size and CTODs at each crack tip in case of three collinear straight cracks.

However, these analyses did not consider the effect of coalescence of yield zones between two small cracks, which may cause the final failure of the structure. Feng and Gross (2000) suggested a fracture criterion for determining the crack propagation for the case of coalescence of collinear cracks in quasi-brittle materials under plane stress conditions. Critical coalescence conditions of plastic zones in an infinite plate was calculated by Nishimura (2000). Bhargava and Hasan (2012) discussed the problem of four collinear straight cracks with coalesced yield zones in an infinite plate under general yielding conditions. Moreover, a number of analytical or numerical methods to predict the residual strength of a cracked plate were proposed in the past. For example, Laurent's expansion method was used by Isida (1965), Complex variable approach by Hasan and Akhtar (2015), Fredholm integral equation method by Chen (1984), Gauss-Chebyshev quadrature method by Chang and Kotousov (2012) and Weight function approach by Xu et al. (2017). Among various mathematical methods, the complex variable method is a convenient and powerful method to solve multiple cracks problems.

In the present paper main consideration will be given on the effect of coalescence of yield zones on the load carrying capacity and crack opening displacement. The mathematical expression is given for stress intensity factor and crack-tip opening displacements ahead of each crack tip when an infinite isotropic plate contains multiple cracks. To do that the complex variable method given by Muskhelishvili (1963) is used. The analytical expressions obtained in the subsequent sections show a good agreement with previously published works for limited cases. Also, a numerical study is carried out to investigate the behavior of yield zone size and CTODs. Graphs are plotted for different crack sizes and different inter crack distances.

2. Formulation of the problem

It is assumed that there are five collinear straight cracks in an infinite isotropic elastic-perfectly plastic plate as shown in Fig. **1**. It is further assumed that the boundary of the plate were subjected to uniform tension stresses σ_∞, resulting the opening of cracks in mode-I deformation and growth of yield zones at each crack tip. However, it should be noted that the yield zones between two outer pairs of cracks were coalesced due increase in tension σ_∞. Therefore, the main objective of this problem is to investigate the load carrying capacity of the plate due to coalescence of yield zones. The developed yield zones are subjected to a constant yield stress distribution, $Y_y = \sigma_{ye}$, to detain further cracks propagation.

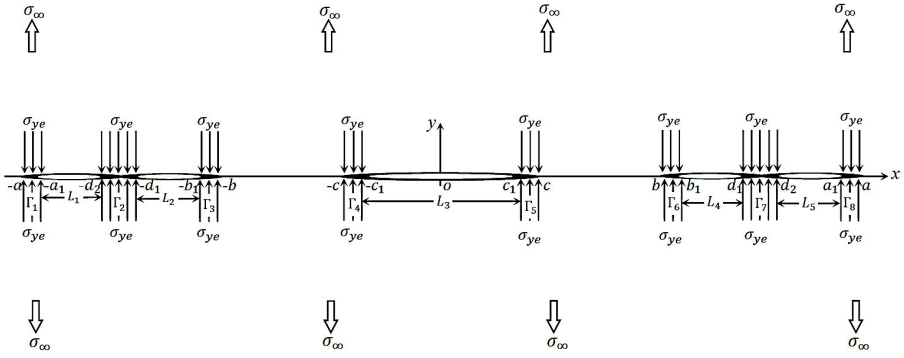

Fig. 1. Configuration of the problem

The entire configuration of the problem is depicted in Fig. 1. Cracks occupy the intervals $L_1 = (-a_1, -d_2)$, $L_2 = (-d_1, -b_1)$, $L_3 = (-c_1, c_1)$, $L_4 = (b_1, d_1)$, $L_5 = (d_2, a_1)$, and yield zones after unification occupy the intervals $\Gamma_1 = (-a, -a_1)$, $\Gamma_2 = (-d_2, -d_1)$, $\Gamma_3 = (-b_1, -b)$, $\Gamma_4 = (-c, -c_1)$,$\Gamma_5 = (c_1, c)$, $\Gamma_6 = (b, b_1)$, $\Gamma_7 = (d_1, d_2)$, $\Gamma_8 = (a_1, a)$ respectively on the x-axis.

3. Solution to the problem

In essence, the solution is obtained by superposing two elastic solutions. The first is that an infinite plate is weakened by three straight cracks which are subject to a normal stress distribution at its boundary. Then second that, five cracks with coalesced yield zones in an infinite plate when the rims of yield zones (including coalesced yield zones) are subject to uniform yield stress distribution.

3.1 Basic solution of the first case (tensile stress distribution)

In this problem we consider three cracks extending from $(-a, -b)$, $(-c, c)$ and (b, a) in an isotropic elastic-perfectly plastic plate associated with the Cartesian system of coordinates xoy. The plate is supposed to be deformed by the opening

of the cracks when the infinite boundary of the plate is subjected to uniform stresses σ_∞. The entire configuration of the problem is depicted in Fig. 2.

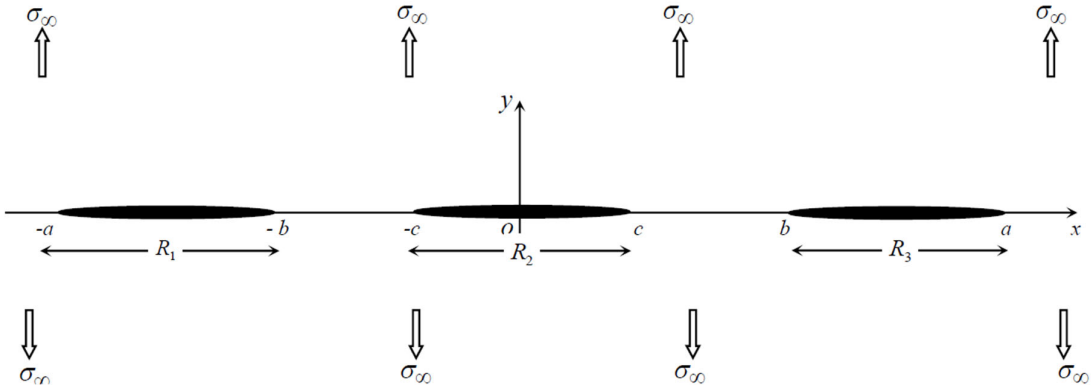

Fig. 2. Configuration of the auxiliary problem - A

The problem is subjected to following boundary conditions

$$Y_y^{\pm} = \sigma_\infty, X_y^{\pm} = 0, \text{for} \quad y \to \pm\infty, -\infty < x < \infty, \tag{1}$$

$$Y_y^{\pm} = X_y^{\pm} = 0, \qquad \text{for} \quad y = 0, x \in \bigcup_{i=1}^{3} R_i, \tag{2}$$

For five cracks with coalesced yield zones in an infinite plate subjected to a remote tension, the stress intensity factor and crack opening displacement of the plate could be obtained by means of complex variable method. Using the boundary conditions (1-2) and the mathematical formulation given in Appendix 1, the desired complex potential function $\Phi_A(\mathrm{z})$ is obtained as:

$$\Phi_A(\mathrm{z}) = \frac{\sigma_\infty}{2}\left[\frac{1}{\chi(\mathrm{z})}\{\mathrm{z}^3 - \mathrm{z}(c^2 + (a^2 - c^2)\lambda_k^2)\} - \frac{1}{2}\right], \tag{3}$$

where subscript A represent the case of first sub-problem and $\chi(\mathrm{z})$, λ_k^2 are defined in Appendix 2.

3.1.1 Stress intensity factor

Opening mode stress intensity factor at the crack tip $\mathrm{z} = \mathrm{z}_1$ is evaluated using the formula given as follows,

$$K^I = 2\sqrt{2\pi}\lim_{\mathrm{z}\to\mathrm{z}_1}\sqrt{\mathrm{z} - \mathrm{z}_1}\Phi(\mathrm{z}). \tag{4}$$

We evaluate the stress intensity factors at each crack tip by substituting $\Phi_A(\mathrm{z})$ from Eq. (3) into Eq. (4). Thus, the analytical expressions for stress intensity factors at crack tips a, b and c can be written as

$$(K_A^I)_a = \sigma_\infty(1 - \lambda_k^2)\sqrt{\frac{\pi a}{k}}, \tag{5}$$

$$(K_A^I)_b = \sigma_\infty\left(\frac{\lambda_k^2}{1 - k^2} - 1\right)\frac{\sqrt{\pi b(1 - k^2)}}{k}, \tag{6}$$

$$(K_A^I)_c = \sigma_\infty\frac{\sqrt{\pi c}}{\sqrt{1 - k^2}}\lambda_k^2. \tag{7}$$

respectively. Superscript I represents the mode-I type deformation.

3.1.2 Components of displacement

The analytical expressions for displacement components v_A due to remotely applied tensile stresses σ_∞ are obtained by using Eq. (3) and Eq. (35) as below relations:

$$v_A^{\pm}(\pm a_1) = \pm\frac{2am\sigma_\infty}{kE}[E(\phi(a_1),k) - \lambda_k^2 F(\phi(a_1),k)], \tag{8}$$

$$v_A^{\pm}(\pm b_1) = \pm\frac{2am\sigma_\infty}{kE}[E(\phi(b_1),k) - \lambda_k^2 F(\phi(b_1),k)], \tag{9}$$

$$v_A^{\pm}(\pm c_1) = \mp\frac{2am\sigma_\infty}{kE}[\rho(\psi(c_1),k) - \lambda_k^2 F(\psi(c_1),k)]. \tag{10}$$

Superscripts $(\pm)$ refer to the values on the upper and lower edge of the cracks. These results may also be taken directly from (Hasan & Akhtar, 2015).

3.2 Basic solution of the second case (closing case)

It is assumed that there are five quasi-static straight cracks located symmetrically on the real axis in an infinite isotropic plate. Yield zones at the tips of outer pairs of cracks get coalesced due to increase in stresses acting at the boundary of the plate. Outer pairs of cracks together with coalesced yield zones are treated as two fictitious cracks. The geometry of the cracked body is shown in Fig . **3**. These yield zones are subjected to uniform stress distribution σ_{ye} whose magnitude is equal to the yield stress of the plate. The basic idea of this stress distribution is to prevent the cracks from further opening.

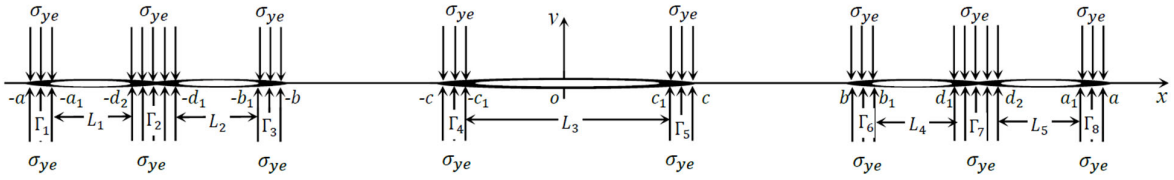

Fig. 3. Configuration of the auxiliary problem - B(Yield Case)

In the present problem, we are considering the case of uniform stress distribution σ_{ye} acting over the rims of yield zones. Then, the boundary conditions for the problem of five cracks with coalesced yield zones are as follows:

$$Y_y = 0, \quad X_y = 0, \text{for} \quad y \to \pm\infty, -\infty < x < \infty, \tag{11}$$

$$Y_y = \sigma_{ye}, \quad X_y = 0, \text{for} \quad y \to 0, x \in \bigcup_{n=1}^{8} \Gamma_n, \tag{12}$$

The desired complex potential function $\Phi_B(\mathrm{z})$ due to coalesced yield zones is obtained by using mathematical formulation given in Appendix 1 and boundary conditions of (11-12) as below equation

$$\Phi_B(\mathrm{z}) = \frac{\sigma_{ye}}{2\pi i\chi(\mathrm{z})}\left[\int_{L'}\frac{\chi(t)dt}{t-\mathrm{z}} + i(D_1\mathrm{z}^2 + D_2\mathrm{z} + D_3)\right], \tag{13}$$

where L' is the union of yield zones including coalesced yield zones. Subscript B stands for second sub-problem.

Using the well known conditions:

$$\chi(t) = \chi(-t) = i\sqrt{a^2-t^2}\sqrt{t^2-b^2}\sqrt{t^2-c^2}, \text{when} \quad -a < t < -b \text{ or } b < t < a, \tag{14}$$

$$\chi(t) = \chi(-t) = -i\sqrt{a^2-t^2}\sqrt{b^2-t^2}\sqrt{c^2-t^2}, \text{when } -c < t < c, \tag{15}$$

Integrals given in Eq. (13) are evaluated using Eq. (14) and Eq. (15) over the rims of yield zones. Thus,

$$\frac{1}{2\mathrm{z}}\int_{L'}\frac{\chi(t)dt}{t-\mathrm{z}} = \int_{a_1}^{a}\frac{\chi(t)}{t^2-\mathrm{z}^2}dt + \int_{b}^{b_1}\frac{\chi(t)}{t^2-\mathrm{z}^2}dt + \int_{d_1}^{d_2}\frac{\chi(t)}{t^2-\mathrm{z}^2}dt + \int_{c_1}^{c}\frac{\chi(t)}{t^2-\mathrm{z}^2}dt, \tag{16}$$

$$= ia^2\left[\frac{m^3}{k}\left\{I_{11}+\left(1-\frac{1}{n^2(\mathrm{z})}\right)H_{11}(\mathrm{z})\right\}-\frac{m_2}{k_2}\left\{I_{22}+\left(1-\frac{1}{n_2^2(\mathrm{z})}\right)H_{22}(\mathrm{z})\right\}\right].$$

Further, the constants D_1, D_2, D_3 given in Eq. (13) are calculated using the condition of single valued of displacement components. Since, the cracks are under symmetric loading condition, therefore, D_1 and D_3 constants are equal to zero and D_2 is evaluated using the Eq. (40) as:

$$D_2 = -\frac{2am}{k}[am^2(J_{11}-\lambda_k^2 J_{12})+c_1\tau(\psi(c_1),k)+\mho_1-\mho_2+\lambda_k^2\mho_3]. \tag{17}$$

Finally, the complex potential function $\Phi_B(\mathrm{z})$ for the second sub-problem is evaluated by substituting Eq. (16) into Eq. (13) as:

$$\Phi_B(\mathrm{z}) = \frac{\mathrm{z}a^2\sigma_{ye}}{\pi\chi(\mathrm{z})}\left[\frac{m^3}{k}\left\{I_{11}+\left(1-\frac{1}{n^2(\mathrm{z})}\right)H_{11}(\mathrm{z})\right\}-\frac{m_2}{k_2}\left\{I_{22}+\left(1-\frac{1}{n_2^2(\mathrm{z})}\right)H_{22}(\mathrm{z})\right\}+\frac{D_2}{2a^2}\right]. \tag{18}$$

3.2.1 Stress intensity factors

Stress intensity factors at each crack tip are extremely important parameters to study the effect of coalesced yield zones on the residual strength of the plate. Therefore, the stress intensity factors at crack tips a, b and c are determined by using Eq. (18) and Eq. (4) as:

$$(K_B^I)_a = \frac{2ak\sigma_{ye}}{m^2\sqrt{a\pi}}\left[\frac{m^3}{k}(I_{11}+H_{11}(a))-\frac{m_2}{k_2}\left\{I_{22}+\left(1-\frac{1}{m_2^2}\right)H_{22}(a)\right\}+\frac{D_2}{2a^2}\right], \tag{19}$$

$$(K_B^I)_b = \frac{-2ak\sigma_{ye}}{m\sqrt{b\pi}\sqrt{1-k_2^2}}\left[\frac{m^3}{k}I_{11}-\frac{m_2}{k_2}\left\{I_{22}+\left(1-\frac{1}{k_2^2}\right)H_{22}(b)\right\}+\frac{D_2}{2a^2}\right], \tag{20}$$

$$(K_B^I)_c = \frac{-2am_2k^2\sigma_{ye}}{m^2\sqrt{c\pi}\sqrt{1-k^2}}\left[\frac{m^3}{k}\left\{I_{11}+\left(1-\frac{1}{k^2}\right)H_{11}(c)\right\}-\frac{m_2}{k_2}I_{22}+\frac{D_2}{2a^2}\right]. \tag{21}$$

3.2.2 Components of Displacement

Opening of cracks take place in mode-I type of deformation due to yield stresses σ_{ye} acting on the rims of the yield zones. Therefore, components of displacement v_B at crack tips $\pm a_1, \pm b_1$ and $\pm c_1$ were calculated using equations (35) and (18). Hence, the analytical expressions of components of displacement are:

$$v_B^{\pm}(\pm a_1) = \mp\frac{2\sigma_{ye}}{\pi E}\left[A_1(\phi(a_1))+A_2(\phi(a_1))-\frac{2kD_2}{am}F(\phi(a_1),k)\right], \tag{22}$$

$$v_B^{\pm}(\pm b_1) = \pm\frac{2\sigma_{ye}}{\pi E}\left[B_1(\varphi(b_1))+B_2(\varphi(b_1))-\frac{2kD_2}{am}F(\varphi(b_1),k)\right], \tag{23}$$

$$v_B^{\pm}(\pm c_1) = \mp\frac{2\sigma_{ye}}{\pi E}\left[C_1(\psi(c_1))+C_2(\psi(c_1))+\frac{2kD_2}{am}F(\psi(c_1),k)\right]. \tag{24}$$

These analytical expressions given in Eqs. (19), (20), (21), (22), (23) and (24) will play an important role for calculating the analytical expressions of applied load ratio and crack tip opening displacement.

4. Analytical Results

In this section, analytical expressions of applied load ratio and crack tip opening displacements are evaluated and written as non-linear equations.

4.1 Size of yield zones

Dugdale hypothesis that the stresses remains finite in the vicinity of each crack tip. Therefore, equating to zero, the stress intensity factors given in Eqs. (5), (6), (7), (19), (20), (21) at the respective crack tip. Hence,

$$(K_A^I)_a + (K_B^I)_a = 0, \quad (K_A^I)_b + (K_B^I)_b = 0, \quad (K_A^I)_c + (K_B^I)_c = 0. \tag{25}$$

As a result, three non-linear equations are obtained.

$$\frac{m^2}{k^2}(1-\lambda_k^2)\left(\frac{\sigma_\infty}{\sigma_{ye}}\right)_a+\frac{2}{\pi}\left[\frac{m^3}{k}(I_{11}+H_{11}(a))-\frac{m_2}{k_2}\left\{I_{22}+\left(1-\frac{1}{m_2^2}\right)H_{22}(a)\right\}+\frac{D_2}{2a^2}\right]=0, \tag{26}$$

$$\frac{m^2}{k^2}(1-k^2-\lambda_k^2)\left(\frac{\sigma_\infty}{\sigma_{ye}}\right)_b+\frac{2}{\pi}\left[\frac{m^3}{k}I_{11}-\frac{m_2}{k_2}\left\{I_{22}+\left(1-\frac{1}{k_2^2}\right)H_{22}(b)\right\}+\frac{D_2}{2a^2}\right]=0, \tag{27}$$

$$\frac{m^2}{k^2}\lambda_k^2\left(\frac{\sigma_\infty}{\sigma_{ye}}\right)_c-\frac{2}{\pi}\left[\frac{m^3}{k}\left\{I_{11}+\left(1-\frac{1}{k^2}\right)H_{11}(c)\right\}-\frac{m_2}{k_2}I_{22}+\frac{D_2}{2a^2}\right]=0. \tag{28}$$

It is almost impossible to determine the yield zone length in terms of applied load ratio. Thus, the yield zone lengths $|a-a_1|, |b_1-b|$ and $|c-c_1|$ are calculated numerically and reported graphically.

4.2 Crack tip opening displacement (CTOD)

Crack-tip opening displacement (CTOD) $\delta(t)$ at crack tips $t=a_1, b_1$ and c_1 is to be determined using the formula given AS follows,

$$\delta(t)=(v_\infty^+(t)+v_{ye}^+(t))-(v_\infty^-(t)+v_{ye}^-(t)). \tag{29}$$

Finally, the mathematical expressions for CTOD at crack tips $x=\pm a_1, \pm b_1, \pm c_1$ are calculated by putting the corresponding values of components of displacements $v_\infty^\pm(t)$ from the equations (8-10) for opening case and $v_{ye}^\pm(t)$ from equations (22-24) for closing case in Eq. (29). After a long mathematical calculation one can obtained,

$$\delta(a_1)=\frac{4\sigma_{ye}}{E}\left[\frac{am}{k}\left(\frac{\sigma_\infty}{\sigma_{ye}}\right)_a\tau(\phi(a_1),k)-\frac{1}{\pi}\left\{A_1(\phi(a_1))+A_2(\phi(a_1))-\frac{2kD_2}{am}F(\phi(a_1),k)\right\}\right], \tag{30}$$

$$\delta(b_1)=\frac{4\sigma_{ye}}{E}\left[\frac{am}{k}\left(\frac{\sigma_\infty}{\sigma_{ye}}\right)_b\tau(\phi(b_1),k)+\frac{1}{\pi}\left\{B_1(\varphi(b_1))+B_2(\varphi(b_1))-\frac{2kD_2}{am}F(\varphi(b_1),k)\right\}\right], \tag{31}$$

$$\delta(c_1)=\frac{4\sigma_{ye}}{E}\left[\frac{am}{k}\left(\frac{\sigma_\infty}{\sigma_{ye}}\right)_c(\lambda_k^2F(\psi(c_1),k)-\rho_2(\psi(c_1),k))-\frac{1}{\pi}\left\{C_1(\psi(c_1))+C_2(\psi(c_1))+\frac{2kD_2}{am}F(\psi(c_1),k)\right\}\right]. \tag{32}$$

5. Verification of analytical expressions

It can be easily verified that the analytical results given in Eq. (26) and Eq. (27) are agreed with the results given by Collins and Cartwright (2001) for two equal cracks taking $c=c_1\to 0$ and $d_1=d_2$, and all the results may also be verified for a limiting case (Hasan & Akhtar, 2015) by taking $d_1=d_2$.

6. Numerical illustration

In order to study the behaviour of yield zone length and CTOD at each crack tip against the applied load ratio, a numerical illustration is presented in the next two subsections. In the first subsection we analyze yield zone length and in second CTOD values.

6.1 Yield zone length

In general, numerical analysis is required to compute the yield zone length using Eqs. (26)-(28) for the case of multiple cracks. In the present analysis, five straight cracks with coalesced yield zone are considered and behaviour of normalized yield zone length against applied load ratio, $\frac{\sigma_\infty}{\sigma_{ye}}$, for different inter-crack distances $\left(\frac{2c_1}{b_1+c_1}=pz\right)$. The value $pz=0.1$ indicates that the fictitious cracks R_1, R_2 and R_3 are situated far away from each other and $pz=0.9$ means that these cracks are situated close to each other. The results from this analysis are presented with help of Figs. 4 to 7.

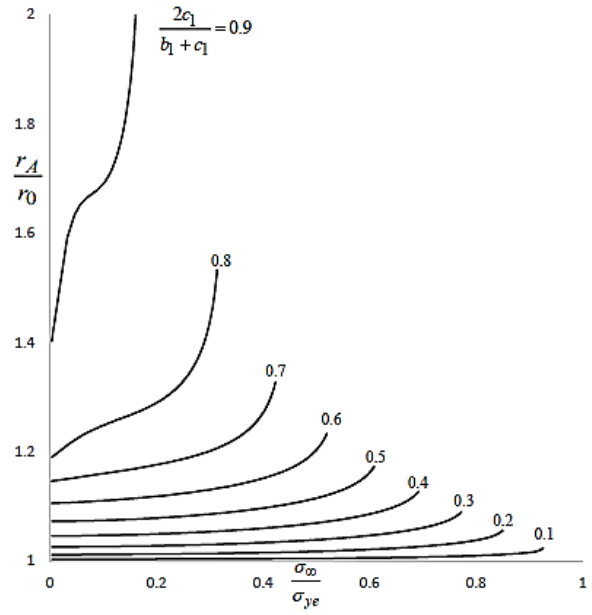

Fig. 4. Variation between $\frac{r_A}{r_0}$ and $\left(\frac{\sigma_\infty}{\sigma_{ye}}\right)_a$

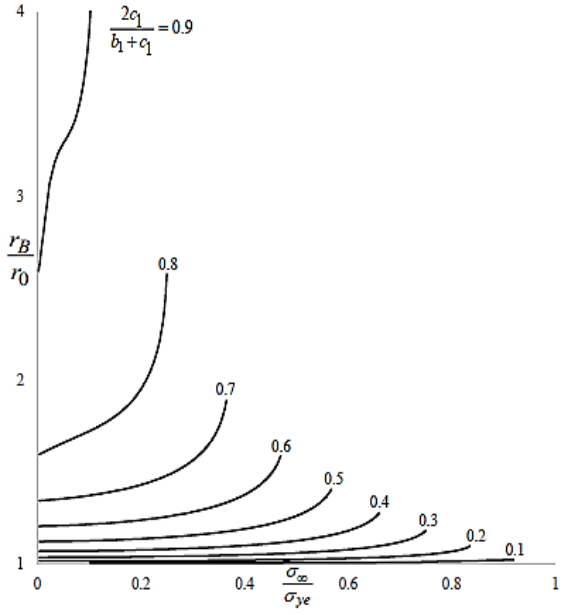

Fig. 5. Variation between $\frac{r_B}{r_0}$ and $\left(\frac{\sigma_\infty}{\sigma_{ye}}\right)_b$

Yield zone length at each crack tip is normalized with the yield zone length of a single Dugdale crack of same length $r_0 = \mathrm{z}\left[\sec\left(\frac{\pi\sigma_\infty}{2\sigma_{ye}}\right)-1\right]$.

Fig. 4 shows the behaviour of normalized yield zone length, $\frac{r_A}{r_0}$ at crack tip a_1, with applied stress ratio for different values of pz, where $r_A = |a - a_1|$. Behaviour of load bearing capacity is studied depending on the positions of cracks. When cracks are situated far away from each other (i.e. $pz = 0.1, 0.2, 0.3$ etc.) effect of applied load on the length of yield zones is negligible. However, a significant increase in yield zone length is seen when cracks are situated close to each other (i.e. $pz = 0.9, 0.8, 0.7$).

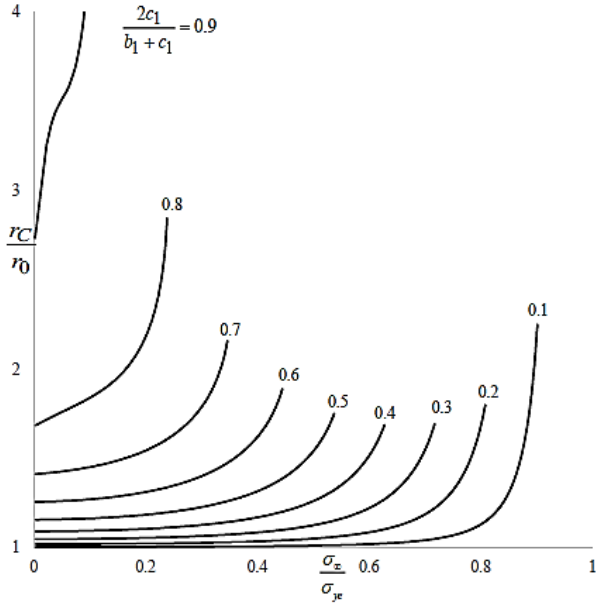

Fig. 6. Variation between $\frac{r_C}{r_0}$ and $\left(\frac{\sigma_\infty}{\sigma_{ye}}\right)_c$

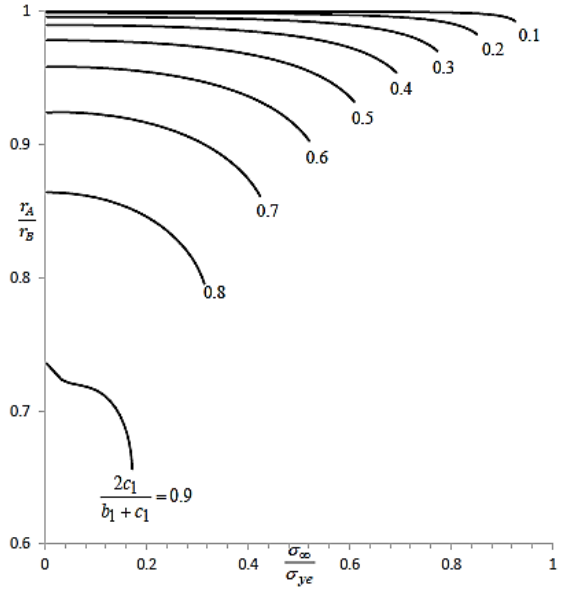

Fig. 7. Variation between $\frac{r_A}{r_B}$ and $\frac{\sigma_\infty}{\sigma_{ye}}$

Normalized yield zone length at the crack tip b, $\frac{r_B}{r_0}$, where $r_B = |b_1 - b|$ is plotted in Fig. 5 against the applied load ratio $\left(\frac{\sigma_\infty}{\sigma_{ye}}\right)_b$. Almost similar behaviour is seen at the crack tip b_1 for $pz = 0.1, 0.2, 0.3$. But, when cracks are situated close to each other (i.e. $pz = 0.9, 0.8, 0.7$) it is seen from the Fig. 1 and Fig. 2 that the yield zone length at the inner crack tip b_1 is much larger as compared to outer tip a_1.

In Fig. 6, the ratio of yield zones $\frac{r_C}{r_0}$, where ($r_C = |c - c_1|$) at crack tip $= c_1$ is plotted against the applied load ratio $\left(\frac{\sigma_\infty}{\sigma_{ye}}\right)_c$. It is observed that the length of normalized yield zone at crack tip c_1 is approximately same to the length of normalized yield zone at crack tip b_1 when applied stress σ_∞ is significantly less than the yield stress σ_{ye} of the plate. However, a remarkable difference in the length of normalized yield zones at both the tips is captured when applied stress is close to yield stress of the plate.

Further, to study the variations in yield zones lengths, ratio of lengths of outer yield zone r_A and inner yield zone r_B with respect to applied stress ratio $\frac{\sigma_\infty}{\sigma_{ye}}$ over a range of crack configurations is depicts in Fig. 7. Almost same yield zone length is seen at outer and inner crack tips of out cracks when these cracks are situated far away from the central crack. On the other hand, the size of yield zone at inner crack tip b_1 is bigger than the yield zone at outer crack tip a_1. This shows that the load bearing capacity is affected by the presence of central crack.

6.2 Crack tip opening displacement

The section deals with the opening of cracks under the applications of remote stresses working at the infinite boundary the plate. Closed form expressions for CTODs are given in Eqs. (30–32) at crack tips a_1, b_1 and c_1, respectively. These results are normalized by the crack tip opening displacement δ_0 of a single isolated Dugdale crack of same length, where $\delta_0 = \frac{8t\sigma_{ye}}{E\pi}\log\left[\sec\left(\frac{\pi\sigma_\infty}{2\sigma_{ye}}\right)\right]$. Variations in CTODs are plotted for different values of the ratio $\left(\frac{2c_1}{b_1+c_1}(\text{say } pz)\right)$. As mentioned earlier, this ratio shows the inter crack distance, means, small value of pz represents that cracks shown in Fig. 2 are situated away from each other. Hence, the cracks do not interact with each other. While the bigger value of pz shows that the cracks are situated close to each other, therefore, it is assume that the cracks interact to each other and this condition influenced the load bearing capacity and opening of cracks as well.

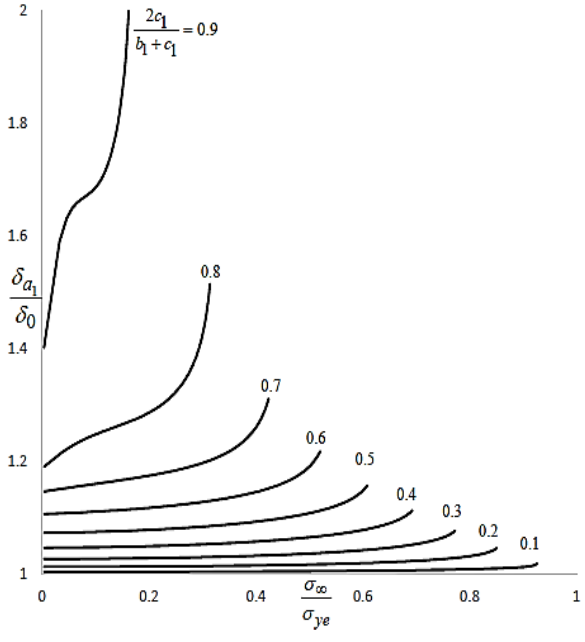

Fig. 8. Variation of $\frac{\delta_{a_1}}{\delta_0}$ with load ratio $\left(\frac{\sigma_\infty}{\sigma_{ye}}\right)_a$

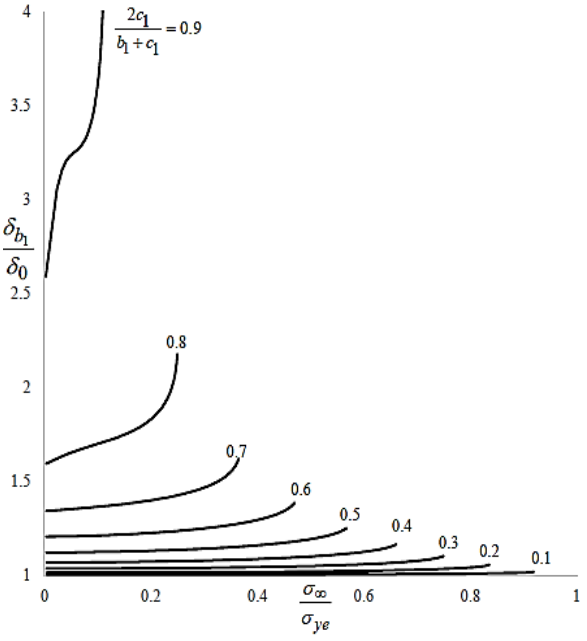

Fig. 9. Variation of $\frac{\delta_{b_1}}{\delta_0}$ with load ratio $\left(\frac{\sigma_\infty}{\sigma_{ye}}\right)_b$

The normalized CTOD at crack tip a_1 has been shown in Fig. 8 against the applied load ratio $\frac{\sigma_\infty}{\sigma_{ye}}$ for different inter-crack distances pz. It can be noticed that the opening of crack at the tip a_1 is approximately equal to the opening of a single isolated central crack of length $2a_1$ when cracks are placed far away from each other. However, a large opening of cracks is seen at

tip a_1 when cracks are situated in close proximity.

Behaviour of opening of crack at the tip b_1 with respect to applied stress ratio has been plotted in Fig. 9. It is noticed that the opening of the crack at tip b_1 more than the crack tip a_1 and single central crack of length $2b_1$ when cracks are placed close to each other ($pz = 0.9,0.8$ etc.). However more or less same opening is seen when $pz = 0.1,0.2$. This shows that the closely located cracks with coalesced yield zones are more catastrophic.

Fig. 10 shows the variation of opening of central crack against the applied stress ratio. Since, inner crack tip is very sensitive due the presence of outer cracks, therefore, it will open more for all values of pz when the applied stress approximately equal to yield stress.

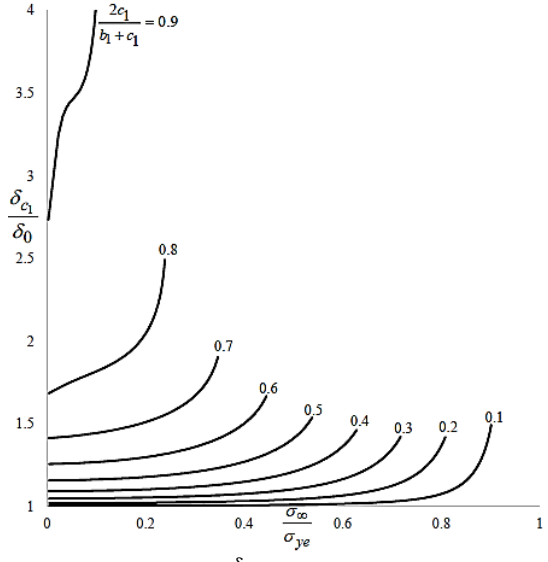

Fig. 10. Variation of $\frac{\delta_{c_1}}{\delta_0}$ with load ratio $\frac{\sigma_\infty}{\sigma_{ye}}$.

7. Conclusion

This paper proposes an analytical model to solve the problem of five collinear straight cracks with unified yield zones in an elastic-perfectly plastic plate. The problem considered in this paper is an extension of Dugdale model (Dugdale, 1960) and may be considered as the prelude situation just before formation of three collinear straight cracks. Analytical expressions of various fracture parameters were obtained after a long and complicated mathematical calculation using Muskhelishvili's complex variable method. Stress intensity factors and crack tip opening displacements were obtained.

Numerical study is carried out in section 6 to investigate the load bearing capacity of the plate for different crack lengths and different inter crack distances. It is observed from the study that the situation when the cracks are located close to each other the plate can bear less load. Also, the opening of yield zones are affected by the presence of other neighbouring cracks. If the crack lengths are much bigger than the inter crack distance, then the yield zone length increases rapidly. On the other side, increase in yield zone length is slow when lengths of cracks are much smaller than the inter crack distance. In case of equal cracks, all the yield zones at each crack tip start to propagate simultaneously, while for the case of unequal cracks the yield zones at the longer cracks propagate slowly in comparison to the shorter crack. Mathematical expressions for parameters stress intensity factors and crack tip opening displacement have been calculated using a complex variable method. On the basis of numerical study carried out in section 6 following conclusion have been made

1. Length of yield zones are almost same at each crack tip a_1, b_1, c_1 when inter crack distance is large, whilst the bigger yield zones are developed at inner crack tips b_1 and c_1 in comparison to outer crack tip a_1.
2. For a fixed yield zone size and fixed value of pz, load carrying capacity of crack tip a_1 is higher in comparison to crack tips b_1 and c_1 both.
3. Furthermore, the unified yield zone $[d_1, d_2]$ makes a significant effect on the load bearing capacity of the plate. Also, when the size of the unified yield zone increases the bearing capacity of the plate also increases.

Appendix 1

Mathematical Formulation

In two dimensional theory of elasticity, components of stresses X_x, Y_y, X_y may be expressed in terms of two complex potential function $\Phi(\mathrm{z}), \Omega(\mathrm{z})$ as

$$X_x + Y_y = 2[\Phi(\mathrm{z}) + \overline{\Phi(\mathrm{z})}], \tag{33}$$

$$Y_y - iX_y = \Phi(\mathrm{z}) + \Omega(\overline{\mathrm{z}}) + (\mathrm{z} - \overline{\mathrm{z}})\overline{\Phi'(\mathrm{z})}, \tag{34}$$

$$2\mu(u + iv) = \kappa\phi(\mathrm{z}) - \omega(\overline{\mathrm{z}}) - (x - \overline{\mathrm{z}})\overline{\Phi(\mathrm{z})}, \tag{35}$$

where bar over the function or variable denotes its complex conjugate.

Consider a homogenous isotropic elastic-perfectly plastic infinite plate weakened by *n* straight cuts L_i (i=1,2,3, n) along *ox*-axis. Let $X_y^{\pm}, Y_y^{\pm}$ be the components of stresses acting over the rims of the cracks. Superscript $(+)$ and $(-)$ denoting the values of stress components on the upper and lower rims of the cracks.

Eqs. (33-34) may be converted into two problems of linear relationship

$$\Phi^+(t) + \Omega^-(t) = Y_y^+ - iX_y^+, \tag{36}$$

$$\Phi^-(t) + \Omega^+(t) = Y_y^- - iX_y^-. \tag{37}$$

under the assumption $\lim_{y\to 0} y\Phi'(t + iy) = 0$.

The general solution of the boundary problems given in Eqs. (36-37) may be written using Sokhotski-Plemelj as:

$$\Phi(\mathrm{z}) + \Omega(\mathrm{z}) = \frac{1}{\pi i\chi(\mathrm{z})}\int_L \frac{\chi(t)p(t)dt}{t - \mathrm{z}} + \frac{2P_n(\mathrm{z})}{\chi(t)}, \tag{38}$$

$$\Phi(\mathrm{z}) - \Omega(\mathrm{z}) = \frac{1}{\pi i}\int_L \frac{q(t)dt}{t - x} - \overline{\Gamma'}, \tag{39}$$

where

$$p(t) = \frac{1}{2}[Y_y^+ + Y_y^-] - \frac{i}{2}[X_y^+ + X_y^-], \quad q(t) = \frac{1}{2}[Y_y^+ - Y_y^-] - \frac{i}{2}[X_y^+ - X_y^-],$$

$$\chi(\mathrm{z}) = \prod_{k=1}^{n}\sqrt{x - a_k}\sqrt{x - b_k}, \quad P_n(\mathrm{z}) = D_0x^n + D_1x^{n-1} + D_2x^{n-2} + \cdots,$$

a_k, b_k denotes the end points of k^{th} crack.

Constants $D_i (i = 0,1,2,..,n)$ shown in $P_n(\mathrm{z})$ are evaluated using loading condition at an infinite boundary of the plate and single-valuedness condition of displacement around the rims of the cracks or cuts,

$$2(\kappa + 1)\int_{L_i}\frac{P_n(t)}{\chi(t)}dt + \kappa\int_{L_i}[\Phi_0^+(t) - \Phi_0^-(t)]dt + \int_{L_i}[\Omega_0^+(t) - \Omega_0^-(t)]dt = 0. \tag{40}$$

where

$$\Phi_0(\mathrm{z}) = \frac{1}{2\pi i\chi(\mathrm{z})}\int_{\cup_{i=1}^n L_i}\frac{\chi^+(t)p(t)}{t - \mathrm{z}}dt + \frac{1}{2\pi i}\int_{\cup_{i=1}^n L_i}\frac{q(t)}{t - \mathrm{z}}dt, \tag{41}$$

$$\Omega_0(\mathrm{z}) = \frac{1}{2\pi i\chi(\mathrm{z})}\int_{\cup_{i=1}^n L_i}\frac{\chi^+(t)p(t)}{t - \mathrm{z}}dt - \frac{1}{2\pi i}\int_{\cup_{i=1}^n L_i}\frac{q(t)}{t - \mathrm{z}}dt. \tag{42}$$

Notes:

- The complex variable formulation given in this section is taken form Muskhelishvili (1963) to make the paper self-understandable.
- All the integrals, involved in the solution of problem, are expressed in the form of elliptic integrals using Byrd and Friedman (1971).

Appendix 2

Used mathematical expressions

$$J_{1i} = j_i(\phi(a_1), m, k) - j_i(\phi(b_1), m, k) + j_i(\phi(b), m, k) + j_i(\phi(d_1), m, k) - j_i(\phi(d_2), m, k),$$
$$J_{2i} = j_i(\vartheta(c_1), m_2, k_2) - j_i(\vartheta(c), m_2, k_2),$$
$$I_{2i} = \ell_i(\vartheta(c_1), m_2, k_2) - \ell_i(\vartheta(c), m_2, k_2),$$
$$I_{1i} = \ell_i(\phi(a_1), m, k) - \ell_i(\phi(b_1), m, k) + \ell_i(\phi(b), m, k) + \ell_i(\phi(d_1), m, k) - \ell_i(\phi(d_2), m, k),$$
$$H_{1i}(x) = h_i(\phi(a_1), m, k, n(x)) - h_i(\phi(b_1), m, k, n(x)) + h_i(\phi(b), m, k, n(x)) + h_i(\phi(d_1), m, k, n(x)) - h_i(\phi(d_2), m, k, n(x)),$$
$$H_{2i}(x) = h_i(\vartheta(c_1), m_2, k_2, n_2(x)) - h_i(\vartheta(c), m_2, k_2, n_2(x)),$$
$$M_1 = M(\phi(a_1), m, k) - M(\phi(b_1), m, k) + M(\phi(b), m, k) + M(\phi(d_1), m, k) - M(\phi(d_2), m, k),$$
$$F_1 = F(\phi_1(a_1), k_1) - F(\phi_1(b_1), k_1) + F(\phi_1(b), k_1) + F(\phi_1(d_1), k_1) - F(\phi_1(d_2), k_1),$$
$$E_1 = E(\phi_1(a_1), k_1) - E(\phi_1(b_1), k_1) + E(\phi_1(b), k_1) + E(\phi_1(d_1), k_1) - E(\phi_1(d_2), k_1),$$
$$\mho_i = w_i(\xi(c_1), k_2, k_1),$$
$$F_2 = F(\vartheta_1(c_1), k_1) - F(\vartheta_1(c), k_1),$$
$$E_2 = E(\vartheta_1(c_1), k_1) - E(\vartheta_1(c), k_1),$$
$$\tau(z,p) = E(z,p) - \lambda_p^2 F(z,p), \quad \lambda_p^2 = \frac{E\left(\frac{\pi}{2}, p\right)}{F\left(\frac{\pi}{2}, p\right)}, \qquad \Lambda(z,p,q) = \frac{\sin 2z\sqrt{1-q^2\sin^2 z}}{4\sqrt{1-p^2\sin^2 z}},$$
$$\rho_2(z,p) = E(z,p) - \tan z\sqrt{1-p^2\sin^2 z}, \quad \rho_1(z,p) = E(z,p) - \frac{\sin z \cos z}{\sqrt{1-p^2\sin^2 z}},$$
$$S(z,p,q) = \frac{p^2 \sin 2z\sqrt{1-q^2\sin^2 z}}{2(1-p^2\sin^2 z)}, \quad \theta_1(z,p) = \tan^{-1}\left[\sqrt{1-p^2}\tan(z)\right],$$
$$M(z,p,q) = \frac{1-q^2}{q^2\sqrt{1-p^2}}\Pi(\theta_1(z,p), q^2, k_1) + \frac{1}{pq}\tan^{-1}\left[\frac{p\, q \sin z \cos z}{\sqrt{1-p^2\sin^2 z}\sqrt{1-q^2\sin^2 z}}\right],$$
$$\sin\phi(t) = \sqrt{\frac{a^2-t^2}{a^2-b^2}}, \quad \sin\phi_1(t) = \frac{b}{t}\sin\big(\phi(t)\big), \quad \sin\psi(t) = \sqrt{\frac{c^2-t^2}{b^2-t^2}},$$
$$\sin\varphi(t) = \frac{1}{k\sin\psi(t)}, \quad \sin\xi(t) = \frac{\sin\psi(t)}{k_2}, \quad \sin\vartheta(t) = \frac{t}{c}, \quad \sin\vartheta_1(t) = \sqrt{\frac{t^2(a^2-c^2)}{c^2(a^2-t^2)}},$$
$$k = \sqrt{\frac{a^2-b^2}{a^2-c^2}}, \quad m = \sqrt{\frac{a^2-b^2}{a^2}}, \qquad k_1 = k \times k_2, \quad k_2 = \frac{c}{b}, \quad m_2 = \frac{c}{a},$$
$$q_1 = \sqrt{\frac{q^2-p^2}{1-p^2}}, \quad r_1 = \sqrt{\frac{r^2-p^2}{1-p^2}},$$
$$n(t) = \sqrt{\frac{a^2-b^2}{a^2-t^2}}, \quad n_1(t) = \frac{1}{\sin\big(\phi_1(t)\big)}, \quad n_2(t) = \frac{c}{t}, \quad n_3(t) = \frac{1}{\sin\big(\psi(t)\big)},$$
$$n_4(t) = \frac{1}{\sin(\varphi(t))}, \quad n_5(t) = \frac{1}{\sin(\vartheta_1(t))},$$
$$\ell_1(z,p,q) = \frac{1}{p^2}[q^2 M(z,p,q) - \ell_2(z,p,q)],$$
$$\ell_2(z,p,q) = \frac{q^2+p^2-p^2q^2}{2}M(z,p,q) + p^2\Lambda(z,p,q) + \frac{\sqrt{1-p^2}}{2}E(\theta_1(z,p), q_1) - \frac{(1-q^2)p^2}{2q^2\sqrt{1-p^2}}F(\theta_1(z,p), q_1),$$
$$\ell_3(z,p,q) = \frac{F(\theta_1(z,p), q_1)}{\sqrt{1-p^2}} - p^2\ell_4(z,p,q),$$
$$\ell_4(z,p,q) = -M(z,p,q) + \frac{1}{q^2\sqrt{1-p^2}}F(\theta_1(z,p), q_1),$$

$$h_1(z,p,q,r) = -q^2M(z,p,q) + \frac{q^2-p^2}{(r^2-p^2)\sqrt{1-p^2}}F(\theta_1(z,p),q_1) + \frac{r^2-q^2}{(r^2-p^2)}h_3(z,p,q,r),$$

$$h_2(z,p,q,r) = (r^2-p^2)h_1(z,p,q,r) + q^2r^2M(z,p,q),$$

$$h_3(z,p,q,r) = \frac{1}{\sqrt{1-p^2}}\Pi(\theta_1(z,p),r_1^2,q_1),$$

$$h_4(z,p,q,r) = \frac{1}{(r^2-p^2)}\left[h_3(z,p,q,r) - \frac{F(\theta_1(z,p),q_1)}{\sqrt{1-p^2}}\right],$$

$$j_1(z,p,q) = \frac{1}{p^2}\left(\ell_2(z,p,q) - E(z,q)\sqrt{1-p^2\sin^2 z}\right),$$

$$j_2(z,p,q) = \frac{1}{p^2}\left(\ell_3(z,p,q) - F(z,q)\sqrt{1-p^2\sin^2 z}\right),$$

$$w_1(z,p,q) = \frac{b}{2}[E(z,q) - (1+k^2-2q^2)F(z,q) - (2q^2-p^2-k^2)\Pi(z,p^2,q) - S(z,p,q)],$$

$$w_2(z,p,q) = b[E(z,q) + k^2(p^2-1)F(z,q) + (p^2-1)(1-k^2)\Pi(z,p^2,q)],$$

$$w_3(z,p,q) = b[F(z,q) + (p^2-1)\Pi(z,p^2,q)],$$

$$T_0(\theta,i,j) = \left(am^2\{I_{11} + M_1(1-k^2)\} + b(E_1+E_2) - \frac{bk}{m}I_{22} - \frac{a^2m^2}{bk^2}(1-k^2)F_1\right)F(\theta,k) - \frac{a^2F_2}{b}\rho_i(\theta,k)$$
$$- \left(am^2M_1 + \frac{c^2}{b}F_1 - \frac{a^2m}{bk}I_{23}\right)\rho_j(\theta,k),$$

$$T_1(\theta,\alpha(z),q) = \frac{kz\chi(z)}{iam(a^2-z^2)}\Pi(\theta,\alpha^2(z),q),$$

$$T_2(\alpha(t)) = 2t^2\Lambda(\phi_1(t),0,k_1)\left(\frac{c^2}{t^2-c^2}F(\varphi(b_1),k) + \frac{t^2}{t^2-b^2}(1-n_3^2(t))\Pi(\varphi(b_1),\alpha^2(t),k)\right),$$

$$T_3(\alpha(t),z) = \frac{2(a^2-t^2)}{t^2-c^2}\Lambda(\vartheta_1(t),0,k_1)(F(z,k) + (n_4^2(t)-1)\Pi(z,\alpha^2(t),k)),$$

$$T_4(t) = 2t^2\Lambda(\phi_1(t),0,k_1)\left(\frac{b^2}{t^2-b^2}F(\psi(c_1),k) + \frac{t^2}{t^2-b^2}(n_3^2(t)-1)\Pi(\psi(c_1),n_3^2(t),k)\right),$$

$$T_5(\alpha(t),z) = \frac{2(a^2-t^2)}{t^2-b^2}\Lambda(\vartheta_1(t),0,k_1)(k^2F(z,k) + (n_3^2(t)-k^2)\Pi(z,\alpha^2(t),k)),$$

$$T_6(x) = \frac{a^2}{bx}[T_1(\phi_1(a_1),n_1(x),k_1) + T_1(\phi_1(d_1),n_1(x),k_1) - T_1(\phi_1(d_2),n_1(x),k_1)] - \frac{m^2}{b}(T_4(a_1) + T_4(d_1) - T_4(d_2)),$$

$$A_1(\theta) = 2[-T_1(\theta,n(a_1),k) + T_1(\theta,n(b_1),k) - T_1(\theta,n(d_1),k) + T_1(\theta,n(d_2),k) - T_1(\theta,n(c_1),k)],$$

$$A_2(\theta) = 4a\Lambda(\theta,0,k)\left(\frac{n^2(a_1)}{\sqrt{1-m^2}}\Pi(\theta_1(\theta,m),n_1^2(a_1),k_1) + n^2(a_1)\big(H_{13}(a_1) - \Pi(\theta_1(\theta,m),n_1^2(a_1),k_1)\big)\right.$$
$$\left. - \frac{m^3n_2^2(a_1)k_2}{km_2}H_{24}(a_1)\right) + 2a\left[E(\theta,k)(I_{13} + \frac{mm_2k_2}{k}I_{24}) - F(\theta,k)(I_{12} - \frac{km_2^3}{mk_2}\{I_{21} + (k_2^2-1)I_{24}\})\right],$$

$$B_1(\theta) = T_0(\theta,2,1) + bm_2^2T_3(n_4(c_1),\theta) - \frac{2m^2b_1^4\Lambda(\phi_1(b_1),0,k_1)}{b(b_1^2-b^2)}(1-n_3^2(b_1))F(\theta,k),$$

$$B_2(\theta) = T_6(b_1) + \frac{a^2}{bb_1}\left[T_1\left(\phi_1(b_1),\frac{k_1}{n_1(b_1)},k_1\right) - \frac{kb_1\chi(b_1)}{iam(a^2-b_1^2)}F(\phi_1(b_1),k_1) - T_1(\vartheta_1(c_1),n_5(b_1),k_1)\right]$$
$$+ \frac{m^2}{b}T_2\left(\frac{k}{n_4(b_1)}\right),$$

$$C_1(\theta) = T_0(\theta,1,2) + \frac{2bm_2^2(a^2-c_1^2)}{c_1^2-b^2}(n_3^2(c_1)-k^2)F(\theta,k) + bm_2^2T_5(n_4(c_1),\theta),$$

$$C_2(\theta) = T_6(c_1) + \frac{a^2}{bc_1}\left[-T_1(\phi_1(b_1),n_1(c_1),k_1) - \frac{kc_1\chi(c_1)}{iam(a^2-c_1^2)}F(\vartheta_1(c_1),k_1) + T_1(\vartheta_1(c_1),\frac{k_1}{n_5(c_1)},k_1)\right] + \frac{m^2}{b}T_4(b_1),$$

References

Barenblatt, G. I. (1962). The mathematical theory of equilibrium cracks in brittle fracture. *Advances in applied mechanics*, *7*, 55-129.

Bhargava, R. R., & Hasan, S. (2012). Crack-tip-opening displacement for four symmetrically situated cracks with coalesced interior yield zones. *Applied Mathematical Modelling*, *36*(11), 5741-5749.

Burdekin, F. M., & Stone, D. E. W. (1966). The crack opening displacement approach to fracture mechanics in yielding materials. *Journal of Strain Analysis*, *1*(2), 145-153.

Byrd, P. F., & Friedman, M. D. (1971). *Handbook of elliptic integrals for engineers and physicists*. Springer.

Chang, D., & Kotousov, A. (2012). A strip yield model for two collinear cracks in plates of arbitrary thickness. *International journal of fracture*, *176*(1), 39-47.

Chen, Y. Z. (1984). Multiple crack problems of antiplane elasticity in an infinite body. *Engineering Fracture Mechanics*, *20*(5-6), 767-775.

Collins, R. A., & Cartwright, D. J. (1996). On the development of the strip yield model for the assessment of multiple site damage. *Theoretical and applied fracture mechanics*, *25*(2), 167-178.

Collins, R. A., & Cartwright, D. J. (2001). An analytical solution for two equal-length collinear strip yield cracks. *Engineering Fracture Mechanics*, *68*(7), 915-924.

Dugdale, D. S. (1960). Yielding of steel sheets containing slits. *Journal of the Mechanics and Physics of Solids*, *8*(2), 100-104.

Feng, X. Q., & Gross, D. (2000). On the coalescence of collinear cracks in quasi-brittle materials. *Engineering Fracture Mechanics*, *65*(5), 511-524.

Findlay, S. J., & Harrison, N. D. (2002). Why aircraft fail. *Materials today*, *5*(11), 18-25.

Harrop, L. P. (1978). Application of a modified Dugdale model to the K vs COD relation. *Engineering Fracture Mechanics*, *10*(4), 807-816.

Hasan, S., & Akhtar, N. (2015). Dugdale model for three equal collinear straight cracks: An analytical approach. *Theoretical and Applied Fracture Mechanics*, *78*, 40-50.

Hasan, S., & Akhtar, N. (2015). Mathematical model for three equal collinear straight cracks: A modified Dugdale approach. *Strength, Fracture and Complexity*, *9*(3), 211-232.

Isida, M. (1966). Stress-intensity factors for the tension of an eccentrically cracked strip.

Kanninen, M. F. (1970). A solution for a Dugdale crack subjected to a linearly varying tensile loading. *International Journal of Engineering Science*, *8*(1), 85-95.

Liu, Z. X., Xu, W., Yu, Y., & Wu, X. R. (2019). Weight functions and stress intensity factors for two unequal-length collinear cracks in an infinite sheet. *Engineering Fracture Mechanics*, *209*, 173-186.

Muskhelishvili, N. I. (1963). *Some Basic Problems of the Mathematical Theory OfElasticity*. P. Noordhoff.

Nishimura, T. (2002). Strip yield analysis of two collinear unequal cracks in an infinite sheet. *Engineering fracture mechanics*, *69*(11), 1173-1191.

Swift, T. (1994). Damage tolerance capability. *International Journal of Fatigue*, *16*(1), 75-94.

Theocaris, P. S. (1983). Dugdale models for two collinear unequal cracks. *Engineering Fracture Mechanics*, *18*(3), 545-559.

Xu, W., & Wu, X. R. (2012). Weight functions and strip-yield model analysis for three collinear cracks. *Engineering Fracture Mechanics*, *85*, 73-87.

Xu, W., Wu, X. R., & Wang, H. (2011). Weight functions and strip yield solution for two equal-length collinear cracks in an infinite sheet. *Engineering fracture mechanics*, *78*(11), 2356-2368.

Xu, W., Wu, X. R., & Yu, Y. (2017). Weight function, stress intensity factor and crack opening displacement solutions to periodic collinear edge hole cracks. *Fatigue & Fracture of Engineering Materials & Structures*, *40*(12), 2068-2079.